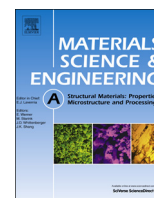




ELSEVIER

Contents lists available at ScienceDirect

## Materials Science &amp; Engineering A

journal homepage: [www.elsevier.com/locate/msea](http://www.elsevier.com/locate/msea)

# Effect of post-solutionizing cooling rate on microstructure and low cycle fatigue behavior of a cast nickel based superalloy

Kumud Kant Mehta<sup>a</sup>, R. Mitra<sup>b,\*</sup>, Sanjay Chawla<sup>a</sup>

<sup>a</sup> Directorate General of Aeronautical Quality Assurance (Materials), C/o-Defence Research and Development Laboratory, Hyderabad 500058, India

<sup>b</sup> Department of Metallurgical and Materials Engineering, Indian Institute of Technology, Kharagpur 721302, India

## ARTICLE INFO

## Article history:

Received 2 November 2013

Received in revised form

1 June 2014

Accepted 3 June 2014

Available online 11 June 2014

## Keywords:

Nickel based superalloy

Post-solutionizing cooling rate

Low cycle fatigue

Precipitates

Bilinear Coffin–Manson relationship

Cyclic stress–strain behavior

## ABSTRACT

The influence of post-solutionizing cooling rate on low cycle fatigue (LCF) and cyclic stress–strain behavior at 650 °C has been investigated for a double solution-treated and aged nickel-based superalloy (Ni–8.09Cr–9.35Co–9.41W–0.52Mo–3.24Ta–0.82Ti–5.51Al–1.53Hf–0.075C). The LCF behavior of this alloy has been characterized by dual-slope Coffin–Manson relationship. The bilinear Coffin–Manson plot for the samples subjected to the slowest post-solutionizing cooling rate has shown relatively lower transition plastic strain for the slope change, and this observation is attributed to their higher cyclic work hardening exponent and more uniform plastic deformation. The increase in amount of cyclic hardening with increasing total strain range and decreasing cooling rate is considered to be due to the increase in dislocation density. The presence of higher volume fraction of fine spherical secondary  $\gamma'$  between the cuboidal primary  $\gamma'$  precipitates, absence of  $\gamma'$ -depleted region near the grain boundaries, and uniform distribution of discrete secondary carbides (such as Cr<sub>23</sub>C<sub>6</sub> and HfC) along the grain boundaries contribute to higher fatigue life and stable cyclic stress–strain behavior for the samples subjected to the slowest cooling rate.

© 2014 Elsevier B.V. All rights reserved.

## 1. Introduction

Cast nickel based superalloys are high performance materials and their importance as hot components of aircraft gas turbine engine has grown several folds during the last four decades. The influence of various constituent alloying elements of well-known nickel based superalloys on their microstructural evolution and mechanical properties has been discussed in several review articles [1–3]. The cast and age-hardenable CM247LC alloy (Ni–8Cr–9Co–9W–5.5Al–3Ta–1.5Hf–0.8Ti–0.5Mo–0.07C) is of interest for use in blades and vanes of aircraft gas turbine, because of its excellent castability, high temperature phase stability, oxidation and corrosion resistance, notch toughness, as well as outstanding tensile, creep and fatigue properties [4]. The aforementioned superalloy is known to have a complex multiphase microstructure containing austenitic (fcc)  $\gamma$ -matrix, L1<sub>2</sub> (ordered fcc) structured coherent  $\gamma'$  precipitates and various types of carbides.

The effects of various types of solutionizing and aging heat-treatments on both microstructural evolution and mechanical properties of the CM247LC alloy have been studied in detail with the objective of finding the optimum heat treatment schedule [4].

However, the variation in microstructures and mechanical properties as function of the post-solutionizing cooling rate (using the optimized temperatures for solution treatment and aging) is not well-understood. Bhowal et al. have shown that size, distribution, and volume fraction of  $\gamma'_c$  (subscript c stands for the  $\gamma'$  precipitates, whose formation takes place during cooling, and volume fraction depends on cooling rate) precipitates strongly depend on both solutionizing temperature and quench severity used for age-hardening heat-treatment of the RENÉ 95 alloy [5]. This study has shown that the average size of  $\gamma'_c$  dispersed in the matrix changes from very fine to coarse with decrease in post-solutionizing cooling rate. Sajjadi et al. [6] have found that size and volume fraction of the  $\gamma'$  precipitates decrease in the UDIMET 500 alloy with increasing post-solutionizing cooling rate. The rate of cooling from the solutionizing temperature also influences the degeneration of primary carbides (MC carbides in as-cast microstructures), which in turn leads to the formation of more stable M<sub>23</sub>C<sub>6</sub> or MC type carbides at the grain boundaries [7].

The hot components of aircraft gas turbines are subjected to cyclic thermal stresses during start-up and shut-down of the engine. The maximum temperature experienced in this thermal cycling process is around 650–700 °C. The life of aircraft gas turbine materials subjected to such thermal cycles can be predicted by carrying out strain-controlled fatigue tests in this temperature range. Therefore, it is important to evaluate the low cycle fatigue (LCF) behavior with emphasis on life prediction and cyclic stress–strain relationship for specific nickel-based superalloys, which are candidate materials for

\* Corresponding author. Tel.: +91 3222 283292; fax: +91 3222 282280.

E-mail address: [rahul@metal.iitkgp.ernet.in](mailto:rahul@metal.iitkgp.ernet.in) (R. Mitra).

use in turbine blades. The LCF behavior is largely influenced by the type of microstructure produced as a result of the extent of quench severity that the superalloy is subjected to during cooling from the solution-treatment temperature [6]. Based on the previously documented results of LCF studies on Nimonic PE16 [8], Nimonic 80A [9], DZ951 [10], IN 718 [11,12] and Waspaloy [13], it has been commonly reported that microstructural variations influence the degree of dislocation–particle-interactions in most of these nickel based superalloys, which in turn result in significant variations in cyclic hardening or softening characteristics as well as low cycle fatigue behavior. In earlier studies, the effects of cyclic frequency [14], strain range [15,16], strain rate [17–19], and test temperatures [20] on cyclic stress-strain response and LCF life have been investigated for different nickel based superalloys.

Based on examination of the literature, it is apparent that optimization of the heat-treatment procedure by choice of suitable post-solutionizing cooling rates is required in order to tailor desirable microstructures in the nickel based superalloys, so that superior mechanical properties are obtained. Therefore, in the present study, an attempt has been made to investigate low cyclic fatigue and cyclic stress strain behavior of the Ni–8Cr–9Co–9W–5.5Al–3Ta–1.5Hf–0.8Ti–0.5Mo–0.07C (equivalent to grade CM247LC) alloy as a function of post-solutionizing cooling rate. The objectives of this work include (i) examination of the relationship of microstructural evolution with post-solutionizing cooling rate; as well as (ii) assessment of the effect of post-solutionized microstructure on tensile properties, cyclic strain hardening/softening behavior, deformation homogeneity, and nature of Coffin–Manson (C–M) plots used to predict the LCF life. Furthermore, the cyclic work hardening coefficients and exponents obtained from the best linear fits of the C–M plots have been correlated with the microstructures of the samples subjected to different post-solutionizing cooling rates.

## 2. Experimental procedure

### 2.1. Processing and heat-treatment

A nickel based superalloy with composition as shown in Table 1 was prepared at Mishra Dhatu Nigam (MIDHANI) Limited, Hyderabad, India, by vacuum induction melting, and then cast into ingots having average diameter of 80 mm. These ingots were remelted in a twin-chambered vacuum melting furnace, and then investment cast into ceramic molds containing 28 equiaxed sample blanks with 12 mm diameter and 125 mm length at the Defense Metallurgical Research Laboratory, Hyderabad, India. Subsequently, the as-cast sample blanks were heat-treated in vacuum following the schedule shown in Table 2. The post-solutionizing cooling rates were varied by introducing argon gas at different pressures in order to induce forced convection. For precise temperature measurements, the thermocouple tip was attached to the samples. Cooling curves depicting the variation of temperature ( $T$ ) with time ( $t$ ) were drawn for each of the aforementioned sample groups. The cooling rate was considered as the slope of the temperature–time plot at 650 °C. This temperature corresponds to the point of inflexion in the plot of  $dT/dt$  against temperature. As shown in Table 2, the samples have been classified into three groups, CR-A, CR-B and CR-C (with 28 samples in each group), on the basis of their cooling rates from the solution-treatment temperature. It is obvious from this table, that the CR-A samples were subjected to the highest cooling rate, whereas CR-B and CR-C were cooled at intermediate and the lowest rates, respectively.

### 2.2. Characterization of microstructure

The specimens for characterization of microstructures were cut from the transverse sections of as-cast and heat-treated sample

**Table 1**

Chemical composition (wt%) of the investigated Ni-based superalloy.

Elements	Ni	Cr	Co	W	Mo	Ta	Ti	Al	Hf	C
Weight %	Bal.	8.09	9.35	9.41	0.52	3.24	0.82	5.51	1.53	0.075

blanks. X-ray diffraction (XRD) studies were carried out in order to identify the phases present in the microstructure of the heat-treated samples. The specimen surfaces were metallographically prepared by grinding and polishing following the standard procedure. Subsequently, the polished surfaces were etched by using freshly prepared Kallings' reagent (5 g  $\text{CuCl}_2$  in a solution containing 40 ml HCl and 60 ml methanol). The constituent phases in the microstructures of the investigated alloys were examined using an environmental SEM (Model FEI Quanta 400) equipped with energy dispersive X-ray analyzer. Furthermore, thin foils were prepared from the heat-treated samples by twin jet thinning using an electrolytic bath containing 78% methanol, 7% sulfuric acid, 10% lactic acid, 3% nitric acid and 2% hydrofluoric acid at  $-30$  °C and 15 mV. The electron transparent specimens prepared in this manner were examined using both bright and dark field TEM imaging methods as well as selected area electron diffraction (SAED) on a transmission electron microscope (TEM, model JEOL JEM 2100, Japan) operated at an acceleration voltage of 200 kV. The specimens subjected to cyclic deformation at different strain amplitudes were sectioned at locations just beneath the fracture surfaces to obtain foils with the surfaces kept normal to their tensile axes. Subsequently, these foils were thinned to achieve electron transparency to carry out TEM studies for understanding the deformation mechanisms operative during the LCF tests.

### 2.3. Low cycle fatigue tests

Low cycle fatigue tests in axial strain control mode under fully reversed pull–push type loading ( $R = -1$ ) condition were conducted using a servo-hydraulic universal testing machine (model DARTEC, M1000/RK, UK) at 650 °C in air till fracture. Strain-controlled LCF tests were carried out following the ASTM E 606-04 standard procedure. The LCF test specimens having gage diameter of 5 mm, parallel length of 16 mm, and shoulder radii of 20 mm were machined from the heat-treated sample blanks. These specimens were prepared with surface finish better than  $0.2 \mu\text{m}$  in both gage and curvature regions, such that circumferential machining marks were absent. The LCF tests were carried out by subjecting the specimens to total axial strain ranges varying between  $\pm 0.2\%$  and  $\pm 0.8\%$  ( $\pm 0.2\%$ ,  $\pm 0.25\%$ ,  $\pm 0.3\%$ ,  $\pm 0.35\%$ ,  $\pm 0.4\%$ ,  $\pm 0.5\%$ ,  $\pm 0.6\%$ ,  $\pm 0.8\%$ ). The strains were measured and controlled by using an axial type ceramic extensometer (Sander, model EXH12-1.25A, Germany) specified for gage length of 10 mm. The strain cycling was carried out at a frequency of 0.3 Hz. The samples were heated inside a 3-zone resistance-heating split furnace (model 3652, Lenton, Thermal Design Ltd., UK) attached to the fatigue testing machine. During LCF testing, the temperature fluctuation near the specimen gage length was maintained within  $\pm 2$  °C using a K-type (chromel–alumel) thermocouple kept very close to the specimen. Three specimens were tested for each strain range to get reproducible results. The cyclic Young's modulus ( $E^*$ ) was determined by subjecting three specimens to strain cycles within the elastic range at 650 °C.

### 2.4. Uniaxial tensile tests

Uniaxial tensile tests were carried out at 650 °C using a screw driven universal testing machine (Instron, model 4507, Wycombe, UK) operated at a nominal strain rate of  $10^{-3} \text{ s}^{-1}$ , using an axial type

Download English Version:

<https://daneshyari.com/en/article/7981018>

Download Persian Version:

<https://daneshyari.com/article/7981018>

[Daneshyari.com](https://daneshyari.com)